Phase formation in the systems Li_2MoO_4–K_2MoO_4–$Ln_2(MoO_4)_3$ (Ln = La, Nd, Dy, Er) and properties of triple molybdates $LiKLn_2(MoO_4)_4$

O.M. Basovich[a], E.G. Khaikina[a],*, S.F. Solodovnikov[b], G.D. Tsyrenova[a]

[a]*Baikal Institute of Nature Management, Siberian Branch, Russian Academy of Sciences, Sakh'yanova Street 6, Ulan-Ude, 670047 Buryat Republic, Russia*
[b]*Nikolaev Institute of Inorganic Chemistry, Siberian Branch, Russian Academy of Sciences, Akad. Lavrent'ev Ave. 3, Novosibirsk 630090, Russia*

Abstract

Subsolidus phase relations in the systems Li_2MoO_4–K_2MoO_4–$Ln_2(MoO_4)_3$ (Ln = La, Nd, Dy, Er) were determined. Formation of $LiKLn_2(MoO_4)_4$ was confirmed in the systems with Ln = Nd, Dy, Er at the $LiLn(MoO_4)_2$–$KLn(MoO_4)_2$ joins. No intermediate phases of other compositions were found. No triple molybdates exist in the system Li_2MoO_4–K_2MoO_4–$La_2(MoO_4)_3$. The join $LiLa(MoO_4)_2$–$KLa(MoO_4)_2$ is characterized by formation of solid solutions.

Triple molybdates $LiKLn_2(MoO_4)_4$ for Ln = Nd–Lu, Y were synthesized by solid state reactions (single phases with ytterbium and lutetium were not prepared). Crystal and thermal data for these molybdates were determined. Compounds $LiKLn_2(MoO_4)_4$ form isostructural series and crystallized in the monoclinic system with the unit cell parameters a = 5.315–5.145 Å, b = 12.857–12.437 Å, c = 19.470–19.349 Å, β = 92.26–92.98°. When heated, the compounds decompose in solid state to give corresponding double molybdates. The dome-shaped curve of the decomposition temperatures of $LiMLn_2(MoO_4)_4$ has the maximum in the Gd–Tb–Dy region.

While studying the system Li_2MoO_4–K_2MoO_4–$Dy_2(MoO_4)_3$ we revealed a new low-temperature modification of $KDy(MoO_4)_2$ with the triclinic structure of α-$KEu(MoO_4)_2$[1] (a = 11.177(2) Å, b = 5.249(1) Å, c = 6.859(1) Å, α = 112.33(2)°, β = 111.48(1)°, γ = 91.30(2)°, space group $P\bar{1}$, Z = 2).

1. Introduction

Existence of the extensive family of the isostructural triple molybdates $LiMR_2(MoO_4)_4$ (M = K, Tl, Rb; R = Bi, Ln) was early reported in [1–4]. Their stability fields shift toward larger R^{3+} cations along with increasing M^+ radius and include Bi, Nd–Lu, Y for the potassium-containing series; Bi, Ce–Eu for the thallium-containing row, and Bi, La–Eu for the rubidium-containing one. The most extensive group of the $LiMR_2(MoO_4)_4$ family is the potassium-containing compounds (13 of 26 representatives). However, whereas information on phase formation in the systems Li_2MoO_4–M_2MoO_4–$R_2(MoO_4)_3$ (M = Tl, Rb) is rather completed [4–6], data for M = K are limited by the system containing bismuth [4].

To fill this gap we undertook the investigation of phase relations in a number of the systems Li_2MoO_4–K_2MoO_4–$Ln_2(MoO_4)_3$ that allowed us to observe a pattern of their changes depending on the nature of a rare-earth element.

*Corresponding author. Fax: +7 3012 434753.
E-mail address: ekha@binm.bsc.buryatia.ru (E.G. Khaikina).
[1]Hereinafter, α refers to a low-temperature modification.

Numerous publications are devoted to phase relations in the boundary binary systems of such triple systems. The phase diagram of the system Li_2MoO_4–K_2MoO_4 was constructed in [7,8]. According to these data the system is characterized by formation of the only intermediate phase $LiKMoO_4$ crystallizing in four polymorphous modifications [9]. Phase equilibria in the systems M_2MoO_4–$Ln_2(MoO_4)_3$ (M = Li, K) are rather complex and change significantly depending on the rare-earth element and the structure of its normal molybdate.

In the systems Li_2MoO_4–$Ln_2(MoO_4)_3$ (Ln = La–Tb) between $Ln_2(MoO_4)_3$ and $LiLn(MoO_4)_2$ with distorted and undistorted scheelite structures, respectively, intermediate phases were found which have an approximate composition $LiLn_5(MoO_4)_8$ with monoclinic scheelite superstructures and wide homogeneity regions. Homogeneity regions of the compounds with an approximate 1:1 composition are also significant. Solid solutions on the base of 1:1 and 1:5 compounds are decomposed peritectically. Subsolidus phase transitions of these compounds are not revealed [10], except of $LiLa(MoO_4)_2$ undergoing an irreversible polymorphous transformation [10,11]. Only β-$LiLa(MoO_4)_2$ possessing the tetragonal scheelite-type structure forms solid solutions [12]. The authors of the latter work suppose that α-$LiLa(MoO_4)_2$ has no appreciable homogeneity region. No intermediate phases were revealed in the lithium containing systems with Ln = Dy–Lu, Y [10] in the range of 50–100 mol% $Ln_2(MoO_4)_3$. Formation of incongruently melting compounds $LiLn(MoO_4)_2$ and $Li_7Ln_3(MoO_4)_8$ with neither noticeable homogeneity regions, nor polymorphism was established. In the system Li_2MoO_4–$Dy_2(MoO_4)_3$, the monotectic reaction $L_2 \leftrightarrow L_1 + \beta$-$Dy_2(MoO_4)_3$ was detected within the range 40–50 mol% Li_2MoO_4.

The systems K_2MoO_4–$Ln_2(MoO_4)_3$ are characterized by formation of a greater number of double molybdates such as $K_5Ln(MoO_4)_4$ and $KLn(MoO_4)_2$ [13–15]. Compounds $K_5Ln(MoO_4)_4$ have no distinct homogeneity regions. While there is a significant structural similarity between $KLn(MoO_4)_2$ and $Ln_2(MoO_4)_3$ based on the scheelite-type structure, 1:1 compounds possess rather extensive homogeneity regions. In this case, as well as in the analogous lithium–lanthanide systems, formation of scheelite-type solid solutions on the base of the phases with an approximate 1:5 composition was determined. When studying the systems with neodymium and europium [13,14] double molybdates $KLn_5(MoO_4)_8$ were obtained. The authors of [13] suggest that $KLn_5(MoO_4)_8$ should exist for the other rare-earth elements forming simple and double molybdates of a 1:1 composition with scheelite-like structures. Nevertheless, despite of scheelite-like structures of $KLa(MoO_4)_2$ and $La_2(MoO_4)_3$, the existence of a similar phase in the potassium–lanthanum system is still uncertain. As it was shown in [15], where T–x diagram of the system K_2MoO_4–$La_2(MoO_4)_3$ was constructed using X-ray powder diffraction and thermal analysis, the obtained results suggested a possible formation of both the intermediate 1:5 phase and the extended solid solution on the base of α-$KLa(MoO_4)_2$. According to [15], only preparation and XRD study of single crystals containing 50 and 83 mol% $La_2(MoO_4)_3$, as well as comparing the types of their superstructures allow us to make the unequivocal conclusion about existence of the 1:5 phase and the character of the phase diagram of this system. In [16,17], the crystals of α- and β-$KLa(MoO_4)_2$ were obtained with hydrothermal crystallization, but their complete structure study was not conducted. The authors of [17] determined that the higher stability limit of the α-modification lies within 560 and 565 °C and indexed the powder pattern of this modification in a body-centered monoclinic subcell with the parameters $a = 5.437(1)$ Å, $b = 12.205(2)$ Å, $c = 5.417(1)$ Å, $\beta = 90.05(1)°$. However, they failed to index a group of the first superstructure reflections. No information on the synthesis of single crystals of $KLa_5(MoO_4)_8$ and its crystal structure is available in literature.

This paper presents results of our studies of subsolidus phase formation in the systems Li_2MoO_4–K_2MoO_4–$Ln_2(MoO_4)_3$ (Ln = La, Nd, Dy, Er) and physicochemical properties of triple molybdates $LiKLn_2(MoO_4)_4$ for Ln = Nd–Lu, Y.

2. Experimental

As starting materials molybdenum trioxide, lithium and potassium carbonates (all reagent grade) and rare-earth oxides with content of the major substance more than 99.9% were taken. Molybdates M_2MoO_4 (M = Li, K) and $Ln_2(MoO_4)_3$ were prepared by solid-state reactions. To avoid a loss of MoO_3 due to its evaporation, annealing was started from 500 °C, stepwise increasing temperature up to 650 °C (to prepare M_2MoO_4) or 750 °C (to obtain rare-earth molybdates). Total duration of solid-state synthesis was 70 h. For better reactivity, the reaction mixtures were ground with ethanol in agate mortars in each 15 h of annealing.

The investigations of interaction in the ternary salt systems were carried out by the "intersecting joins" method [18,19]. The method is based on determination of phase compositions of the interception points of all joins connecting the composition points of the components, binary and ternary compounds. Using X-ray powder diffraction we revealed quasibinary sections to construct triangulated phase diagrams of the systems Li_2MoO_4–K_2MoO_4–$Ln_2(MoO_4)_3$.

X-ray diffraction analysis (XRD) was performed on a diffractometer DRON-UM1 (Cu$K\alpha$-radiation). In the most important cases such as determining homogeneity

range limits, XRD patterns were recorded with an Enraf-Nonius FR-552 focusing camera (Cu$K\alpha_1$-radiation, quartz monochromator, Ge as internal standard). The same camera was also used to determine unit cell parameters of the obtained phases. Differential thermal analysis was performed with an MOM OD-103 derivatograph.

3. Results and discussion

3.1. Phase equilibria in the systems Li_2MoO_4–K_2MoO_4–$Ln_2(MoO_4)_3$ ($Ln = La, Nd, Dy, Er$)

3.1.1. Binary boundary systems

We have confirmed literature data [7–10,13–16,20–26] on existence of double molybdates LiKMoO$_4$, $MLn(MoO_4)_2$ ($M = $ Li, K; $Ln = $ La, Nd, Dy, Er), $Li_7Ln_3(MoO_4)_8$ ($Ln = $ Dy, Er), $LiLn_5(MoO_4)_8$ ($Ln = $ La, Nd), $K_5Ln(MoO_4)_8$ ($Ln = $ La, Nd, Dy, Er), $KNd_5(MoO_4)_8$ in the systems Li_2MoO_4–K_2MoO_4 and M_2MoO_4–$Ln_2(MoO_4)_3$ ($M = $ Li, K; $Ln = $ La, Nd, Dy, Er). Following recommendations [9,10,12,16,20,21,27], these phases were synthesized using solid-state reactions and further taken for phase formation studies in the ternary salt systems Li_2MoO_4–K_2MoO_4–$Ln_2(MoO_4)_3$ ($Ln = $ La, Nd, Dy, Er). Crystal and thermoanalytical characteristics of the double molybdates obtained agree well with the results of the last publications.

3.1.2. Subsolidus phase formation in the systems Li_2MoO_4–K_2MoO_4–$Ln_2(MoO_4)_3$ ($Ln = La, Nd, Dy, Er$)

The results of experimental studies of the ternary systems Li_2MoO_4–K_2MoO_4–$Ln_2(MoO_4)_3$ ($Ln = $ La, Nd, Dy, Er) are presented in Fig. 1. Formation of triple molybdates LiKLn_2(MoO$_4$)$_4$ having no distinct homogeneity regions was confirmed in the systems with $Ln = $ Nd, Dy, Er in the quasibinary sections LiLn(MoO$_4$)$_2$–KLn(MoO$_4$)$_2$. The directions of other triangulating joins primarily defined by phase formation in the binary boundary systems. Thus, the systems with dysprosium and erbium having similar boundary systems are divided by the quasibinary joins K_5Ln(MoO$_4$)$_4$–LiKMoO$_4$, KLn(MoO$_4$)$_2$–LiKMoO$_4$, KLn(MoO$_4$)$_2$–Li$_2$MoO$_4$, KLn(MoO$_4$)$_2$–LiKLn_2(MoO$_4$)$_4$, LiKLn_2(MoO$_4$)$_4$–LiLn(MoO$_4$)$_2$, LiKLn_2(MoO$_4$)$_4$–Li$_2$MoO$_4$, LiKLn_2(MoO$_4$)$_4$–Li$_7Ln_3$(MoO$_4$)$_8$, LiKLn_2(MoO$_4$)$_4$–Ln_2(MoO$_4$)$_3$ into 8 secondary triangles.

An analogous subsolidus triangulation was found for the region Li$_2$MoO$_4$–K$_2$MoO$_4$–KNd(MoO$_4$)$_2$–LiNd(MoO$_4$)$_2$ of the ternary system Li$_2$MoO$_4$–K$_2$MoO$_4$–Nd$_2$(MoO$_4$)$_3$. A little difference is determined only by lack of the 7:3 phase in the system Li$_2$MoO$_4$–Nd$_2$(MoO$_4$)$_3$. It should be noted that we have
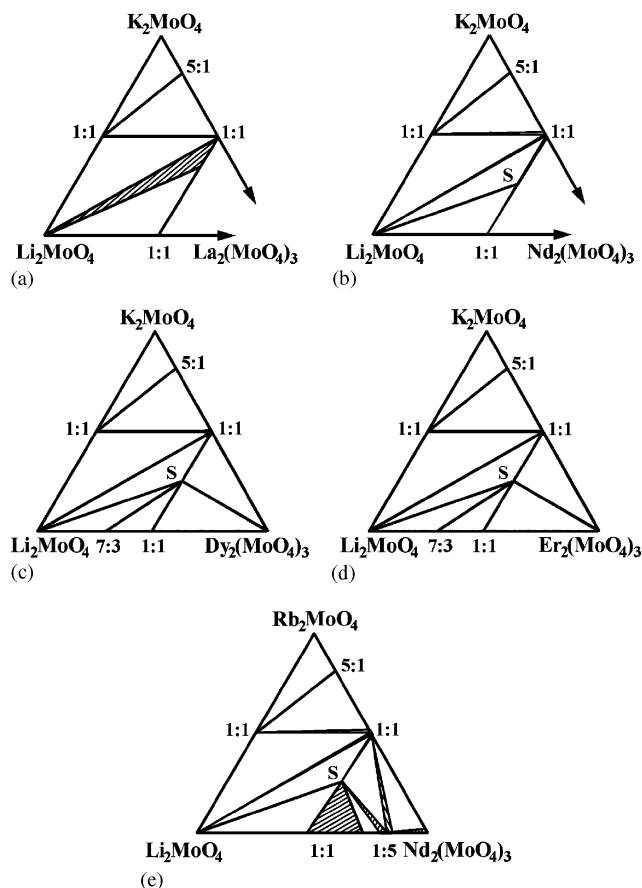

Fig. 1. Subsolidus phase diagrams of some Li_2MoO_4–M_2MoO_4–Ln_2 $(MoO_4)_3$ systems ($M = $ K, $t = $ 500–550 °C; $M = $ Rb, $t = $ 600 °C). S = LiMLn_2(MoO$_4$)$_4$.

been revealed the similar quasibinary sections [5] in the Li–Rb–Nd molybdate system (Fig. 1e).[2]

The correct study of the region KNd(MoO$_4$)$_2$–LiNd (MoO$_4$)$_2$–Nd$_2$(MoO$_4$)$_3$ is troublesome. Identification of intermediate phases in this region is rather complicated by a similarity of their scheelite-type superstructures, especially for LiNd$_5$(MoO$_4$)$_8$, KNd$_5$(MoO$_4$)$_8$ and Nd$_2$(MoO$_4$)$_3$. As a result, we failed to determine the strict phase limits in the region KNd(MoO$_4$)$_2$–LiNd (MoO$_4$)$_2$–Nd$_2$(MoO$_4$)$_3$ and decided to omit such uncertain data from the paper. However, we would like to emphasize that LiKLn_2(MoO$_4$)$_4$ are the only triple molybdates which were detected in all the three systems Li$_2$MoO$_4$–K$_2$MoO$_4$–Ln_2(MoO$_4$)$_3$ ($Ln = $ Nd, Dy, Er).

As it was mentioned above, existence of KLa$_5$ (MoO$_4$)$_8$ in the system K$_2$MoO$_4$–La$_2$(MoO$_4$)$_3$ is still under discussion. A more thorough study of intermediate phases in the range 50–100 mol% La$_2$(MoO$_4$)$_3$ and preparation of their single crystals are beyond the scope

---

[2]When published a misprint was made in the phase equilibria scheme of the system Li$_2$MoO$_4$–Rb$_2$MoO$_4$–Nd$_2$(MoO$_4$)$_3$ [5]. This paper gives the correct version of the figure.

of our work. Thus, we decided to investigate the system Li_2MoO_4–K_2MoO_4–$La_2(MoO_4)_3$ only in the region Li_2MoO_4–K_2MoO_4–$KLa(MoO_4)_2$–$LiLa(MoO_4)_2$ (Fig. 1a). The most attention is paid to phase equilibria in the section $LiLa(MoO_4)_2$–$KLa(MoO_4)_2$ where we would expect to form a phase analogous to triple molybdates $LiMLn_2(MoO_4)_4$ found in the systems with Nd, Dy and Er (Figs. 1b,c, and d). While studied this section, as initial substances were taken the low-temperature forms of the double molybdates, the orthorhombic modification of $LiLa(MoO_4)_2$ and the monoclinic one of $KLa(MoO_4)_2$, whose X-ray characteristics corresponded to literature data [11,17]. It was established that interaction between $LiLa(MoO_4)_2$ and $KLa(MoO_4)_2$ resulted in formation of solid solutions. Solubility of $LiLa(MoO_4)_2$ in $KLa(MoO_4)_2$ is about 30 mol% at 500 °C and extends considerably at more elevated temperatures. At 600 °C, solid solutions become bilateral. At the temperatures higher than the points of phase transitions into high-temperature modifications of the undistorted scheelite-type structure, the formation of the continuous series of solid solutions was observed. Thus, we confirmed the absence of $LiKLa_2(MoO_4)_4$ as well as other triple molybdates in this system under the conditions studied.

3.2. New modification of $KDy(MoO_4)_2$

XRD analysis of the system Li_2MoO_4–K_2MoO_4–$Dy_2(MoO_4)_3$ at 400–500 °C in the sections $KDy(MoO_4)_2$–$LiKMoO_4$, $KDy(MoO_4)_2$–Li_2MoO_4, $KDy(MoO_4)_2$–$LiKDy_2(MoO_4)_4$ as well as three-phase regions bordered by these sections was revealed the reflections of an unknown phase. Since the XRD patterns were similar to those of triclinic α-modifications $KLn(MoO_4)_2$ (Ln = Eu–Tb) and intensities of the reflections increased with approaching the compositions of the reaction mixtures to $KDy(MoO_4)_2$, we assigned the unknown lines to a new polymorphous modification of $KDy(MoO_4)_2$.

The most $KLn(MoO_4)_2$ are known to possess a developed polymorphism. Depending on different rare-earths and formation conditions, 9 structure types were identified [24,25,28–30]. The greatest number of polymorphous modifications were found for $KLn(MoO_4)_2$ in the middle of the lanthanide series. For instance, both $KEu(MoO_4)_2$ and $KGd(MoO_4)_2$ have 5 polymorphous modifications under atmospheric pressure [28]. On the other hand, according to recent publications [24,25,29,30] $KLn(MoO_4)_2$ (Ln = Dy, Y, Ho, Er, Tm) have no phase transformations above room temperature up to the melting points under atmospheric pressure.

In order to evidence polymorphism in $KDy(MoO_4)_2$ numerous attempts were undertaken to synthesize this compound under different conditions as well as performing careful studies of phase compositions of the

sections $KDy(MoO_4)_2$–$LiKMoO_4$, $KDy(MoO_4)_2$–Li_2MoO_4 and $KDy(MoO_4)_2$–$LiKDy_2(MoO_4)_4$ near $KDy(MoO_4)_2$ with 0.5 mol% step. When studying sections, ternary reaction mixtures Li_2MoO_4, K_2MoO_4, $Dy_2(MoO_4)_3$ or $LiKMoO_4$, K_2MoO_4, $Dy_2(MoO_4)_3$ as starting reactants were taken. $KDy(MoO_4)_2$ was synthesized from both simple molybdates and thermally less stable reactants such as nitrates and carbonates.

Samples of the $LiKMoO_4$–$KDy(MoO_4)_2$ section in vicinity of $KDy(MoO_4)_2$ annealed at 400–500 °C for 50 h were single-phase independently on the nature of starting reagents. Powder patterns of the samples were successfully indexed suggesting the phase to be isostructural to low-temperature triclinic α-$KEu(MoO_4)_2$. XRD analysis results of a specimen with composition $0.99KDy(MoO_4)_2 \cdot 0.01LiKMoO_4$ are given as an example in Table 1. Unit cell parameters of the samples containing more than 2 mol% $LiKMoO_4$ are the same within the error of measurement. This allowed us to estimate the extension of the solid solution on the base of $KDy(MoO_4)_2$ along the $LiKMoO_4$–$KDy(MoO_4)_2$ section being equal to ~2 mol%.

A number of attempts to detect the α-$KEu(MoO_4)_2$-type phase directly in undoped samples of $KDy(MoO_4)_2$ were successful that gave the undoubted evidence of polymorphism of this compound. The new form is a low-temperature one transforming into the high-temperature orthorhombic modification above 550 °C. Triclinic α-$KDy(MoO_4)_2$ crystallizes in the space group $P\bar{1}$, $Z = 2$ and has the unit cell dimensions: $a = 11.177(2)$ Å, $b = 5.249(1)$ Å, $c = 6.859(1)$ Å, $\alpha = 112.33(2)°$, $\beta = 111.48(1)°$, $\gamma = 91.30(2)°$.

Nevertheless, it should be emphasized that we failed to prepare single-phase samples of the triclinic form of undoped K-Dy-molybdate: we always find the latter along with predominant amounts of the orthorhombic modification of the $KY(MoO_4)_2$ - type (Table 1) well-documented in literature [26,29,31]. The doping and solid solution formation seem to be factors to stabilize the triclinic modification. Moreover, annealing of mixtures $LiKMoO_4$, $KDy(MoO_4)_2$, or Li_2MoO_4, $KDy(MoO_4)_2$, or $KDy(MoO_4)_2$, $LiKDy_2(MoO_4)_4$ containing the orthorhombic form of K-Dy-molybdate at 400–450 °C results in the transformation of the latter in the new triclinic form, suggesting reversibility of the transition. We failed to observe the reversible transformation for undoped $KDy(MoO_4)_2$. The solubility of Li_2MoO_4 and $LiKDy_2(MoO_4)_4$ in $KDy(MoO_4)_2$ does not exceed 2 and 1 mol%, respectively, at 500 °C. But it is sufficient to stabilize the triclinic α-modification, which is observed in the sections $KDy(MoO_4)_2$–Li_2MoO_4 and $KDy(MoO_4)_2$–$LiKDy_2(MoO_4)_4$ along with β-$KDy(MoO_4)_2$.

The obtained experimental data on stabilization of the new modification of $KDy(MoO_4)_2$ by lithium doping can be indirectly confirmed by an analysis of probable

Table 1
Results of the XRD studies of some samples of the KDy(MoO$_4$)$_2$–LiKMoO$_4$ section

KDy(MoO$_4$)$_2$ (experimental sample)		0.99KDy(MoO$_4$)$_2$ · 0.01LiKMoO$_4$		KDy(MoO$_4$)$_2$ (α-KEu(MoO$_4$)$_2$ structure type, theoretical XRD pattern)[a]					KDy(MoO$_4$)$_2$ (KY(MoO$_4$)$_2$ structure type), [31][b]	
$2\theta°$	I/I_0	$2\theta°$	I/I_0	$2\theta°$	I/I_0	h	k	l	$2\theta°$	I/I_0
8.667	60	8.674	100	8.649	100	1	0	0		
9.738	100								9.728	100
14.168	3	14.167	5	14.167	4	−1	0	1		
14.773	1								14.770	2
15.270	<1	15.305	1	15.263	1	0	0	1		
17.332	<1	17.332	1	17.347	1	2	0	0		
17.883	1	17.873	2	17.880	1	−2	0	1		
18.088	<1								18.092	1
18.542	1	18.544	2	18.493	1	0	−1	1		
				18.590	1	0	1	0		
18.993	<1	19.035	1	18.984	1	−1	1	0		
19.285	<1	19.275	<1	19.254	1	−1	−1	1		
19.562	<1								19.531	1
20.416	2	20.404	3	20.426	3	1	0	1		
21.272	<1								21.266	1
21.582	<1	21.577	3	21.578	3	1	−1	1		
22.016	2	21.990	3	21.983	3	1	1	0		
22.239	<1								22.264	1
22.816	40								22.810	27
24.333	2	24.349	2	24.345	2	−3	0	1	24.351	1
25.416	5								25.428	4
27.070	3	27.065	5	27.031	4	−1	1	1		
				27.091	4	−1	−1	2		
27.284	30	27.284	60	27.286	63	2	−1	1		
27.872	30	27.866	60	27.868	54	2	1	0		
28.122	30	28.129	60	28.112	61	−2	1	1		
				28.358	3	−1	0	2		
28.433	30	28.445	60	28.421	62	−2	−1	2		
28.522	<1	28.550	<1	28.556	1	0	−1	2		
				28.557	<1	−2	0	2		
		28.733	<1	28.748	1	0	1	1		
28.856	60								28.846	49
29.216	<1	29.207	2	29.196	2	−3	1	0		
29.462	<1								29.483	2
29.759	30								29.793	25
		29.818	1	29.860	1	−3	−1	1		
30.186	40								30.210	36
30.803	15	30.812	30	30.806	30	0	0	2		
31.732	2	31.752	5	31.727	4	−3	1	1		
32.036	10	32.033	20	32.037	25	−4	0	1		
32.246	1	32.246	3	32.229	4	−3	−1	2		
34.158	10	34.158	20	34.143	22	0	−2	1		
34.415	2	34.402	5	34.432	5	3	−1	1		
35.100	5	35.103	10	35.079	2	1	−2	1		
				35.114	8	3	1	0		
35.278	5								35.263	5

[a]The theoretical XRD pattern was calculated with the RIETAN-94 program [32]. Coordinates of the basis atoms in the prototype structure were taken from [33]. The unit cell parameters (see the text) were obtained as a result of the X-ray powder diffraction pattern indexing of KDy(MoO$_4$)$_2$ experimental sample. Reflexes from $I/I_0 < 0.4$ are not given in the table.
[b]Reflexes from $I/I_0 < 1$ are not given in the table.

cavities in the crystal structure of α-KEu(MoO$_4$)$_2$ [33]. The analysis was carried out with the CAVITY package [34], which allowed tetrahedral and more extended cavities to be detected in the structure using the given atomic radii. In the unit cell of α-KEu(MoO$_4$)$_2$ there are five large cavities with CN = 4 (one void), 6 (one void) and 7 (three voids) with the distances 1.9–2.5 Å from their centers to oxygen vertices. The cavity with CN = 6 (Fig. 2) appears to be the most suitable for lithium insertion. Thus, an unusual stabilizing influence of

lithium doping can be positively explained as the formation of an interstitional/substitutional solid solution on the base of α-KDy(MoO$_4$)$_2$ with distinct homogeneity regions. In this case, the probable general formulae of the solid solutions can be written as:

(i) Li$_{2x}$(K$_{1-x}$Li$_x$)(Dy$_{1-x}$Li$_x$)(MoO$_4$)$_2$ in the section KDy(MoO$_4$)$_2$–Li$_2$MoO$_4$;

(ii) Li$_{2x}$K(Dy$_{1-x}$K$_x$)(MoO$_4$)$_2$ in the section KDy (MoO$_4$)$_2$–LiKMoO$_4$.

It is worth to note that there is a kind of a precedent for the observed insertion: triple molybdates LiRbBi$_2$ (MoO$_4$)$_4$ [35] and Li$_3$Ba$_2$Ln$_3$(MoO$_4$)$_8$ [36] can be considered as derivatives of the BaNd$_2$(MoO$_4$)$_4$-type structure [37] with lithium insertion into its vacant crystallographic positions.

The attempts to obtain modifications of the α-KEu(MoO$_4$)$_2$ type for double molybdates KLn(MoO$_4$)$_2$ containing rare-earths close to dysprosium in ionic radii (Ln = Y, Ho, Er) were unsuccessful.

Our results slightly extend the existence region of the triclinic α-KEu(MoO$_4$)$_2$ structure toward the heavy lanthanides. Trends in changing the unit cell parameters and volumes of double molybdates α-KLn(MoO$_4$)$_2$ in the rare-earth series observed early for Ln = Eu, Gd, Tb keep for Dy (Table 2, Fig. 3).

3.3. Triple molybdates LiKLn$_2$(MoO$_4$)$_4$ (Ln = Nd–Lu, Y)

Solid-state synthesis of single-phase triple molybdates LiKLn$_2$(MoO$_4$)$_4$ (Ln = Nd–Tm, Y) were performed by annealing of stoichiometric mixtures Li$_2$MoO$_4$, K$_2$MoO$_4$, Ln$_2$(MoO$_4$)$_3$ or LiKMoO$_4$, Ln$_2$(MoO$_4$)$_3$ at 500–550 °C for 40–80 h. Formation rates of such phases in the rare-earth series seems to decrease that may be a reason why we failed to obtain single-phase compounds with Yb and Lu despite of our attempts to vary temperature and time conditions in rather wide ranges.

Compounds LiKLn$_2$(MoO$_4$)$_4$ decompose in solid state to give the corresponding double molybdates. A similar behavior is observed for isoformular rubidium and thallium containing triple molybdates of lanthanides. When heated, LiMCe$_2$(MoO$_4$)$_4$ (M = Rb, Tl) show in some way other behavior, decomposing with partial oxidation of Ce^{3+} to Ce^{4+} [2,3,5]. As seen in Figs. 4a and b, thermal stability of rubidium containing phases are higher compared with thallium containing triple molybdates. The dome-shaped curve showing the

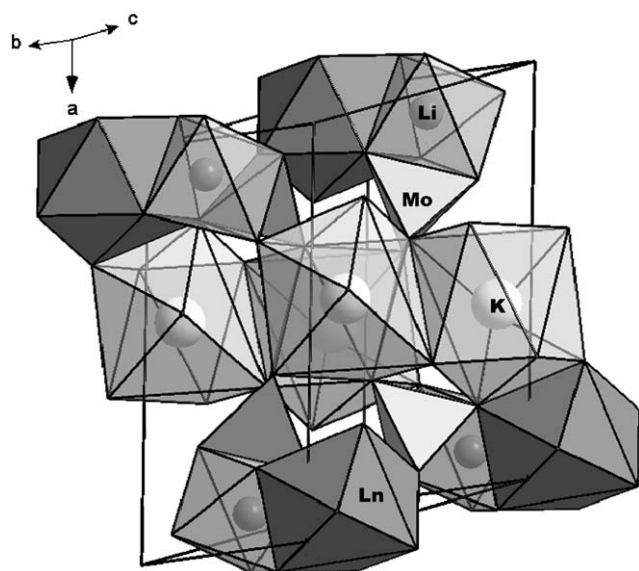

Fig. 2. Possible arrangement of inserted Li$^+$ ions in octahedral voids of the KLn(MoO$_4$)$_2$ with the triclinic KEu(MoO$_4$)$_2$ structure.

Table 2
Crystallographic characteristics of KLn(MoO$_4$)$_2$ with the α-KEu(MoO$_4$)$_2$ structure

Ln	a (Å)	b (Å)	c (Å)	α (deg)	β (deg)	γ (deg)	V/Z (Å)^3	Reference
Eu	12.82	11.21	10.59	90.88	90.10	114	173.8	[38]
	11.21	5.295	6.94	112.53	111.71	90.88[a]		
	12.79	5.29	11.19	91	114	90	172.9	[28]
	11.19	5.29	6.92	112.5	111.7	91.0[b]		
	11.20(3)	5.30(1)	12.81(3)	90(0.5)	114(0.5)	91(0.5)	173.6	[33]
	11.20	5.30	6.94	112.5	111.5	91		
Gd	12.78	11.19	10.56	91.17	89.97	113.92	172.5	[38]
	11.19	5.275	6.91	112.40	111.53	91.17[a]		
	12.79	5.29	11.19	91	114	90	172.9	[28]
	11.19	5.29	6.92	112.5	111.7	91.0[b]		
Tb	12.73	11.19	10.53	91.18	89.87	113.87	171.4	[38]
	11.19	5.265	6.88	112.36	111.49	91.18[a]		
Dy	11.177(2)	5.249(1)	6.859(1)	112.33(2)	111.48(1)	91.30(2)	170.10	Our data

[a]Parameters were calculated by matrix 0 1 0/0 0 0.5/0.5 0 −0.25.

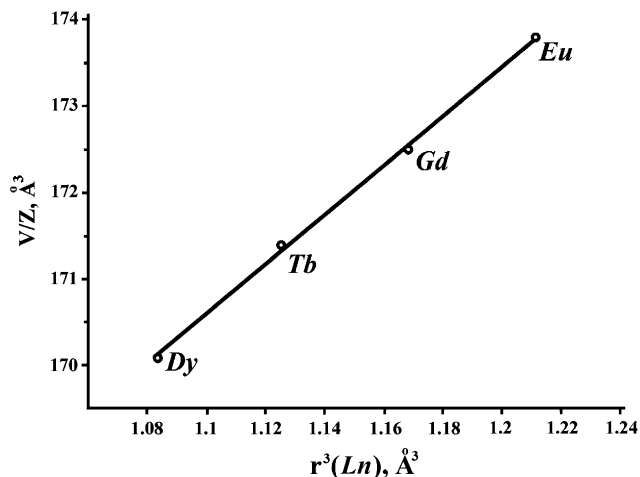[b]Parameters were calculated by matrix 0 0 −1/0 −1 0/−0.5 0.5 0.

Fig. 3. V/Z dependence on $r^3(Ln)$ for a α-KLn(MoO$_4$)$_2$ (Ln = Eu–Dy). While calculating V/Z for α-KLn(MoO$_4$)$_2$ (Ln = Eu–Tb) the data [38] were used, Ln^{3+} radii for CN = 8 were taken from [39].
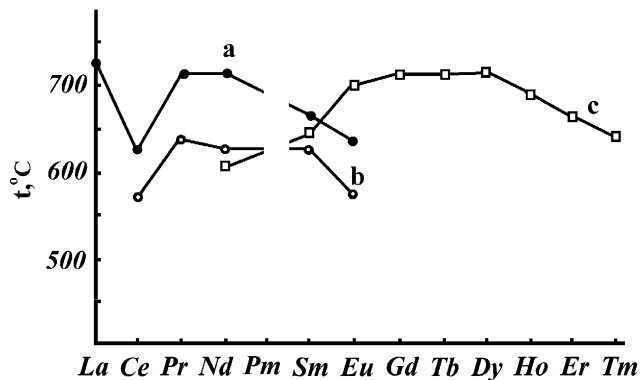

Fig. 4. Dependence of decomposition temperatures of LiMLn_2 (MoO$_4$)$_4$ on the atomic number of a lanthanide: a—LiRbLn_2(MoO$_4$)$_4$; b—LiTlLn_2(MoO$_4$)$_4$, c—LiKLn_2(MoO$_4$)$_4$. Data for LiMLn_2(MoO$_4$)$_4$ (M = Rb, Tl, in part K) were taken from [2,3].

Fig. 5. Projection of the crystal structure of LiMLn_2(MoO$_4$)$_4$ on to the yz plane [40].

Table 3
Crystallographic characteristics of LiKLn_2(MoO$_4$)$_4$

Ln	Unit cell parameters				
	a (Å)	b (Å)	c (Å)	β (deg)	V (Å)^3
Nd	5.315(1)	12.857(1)	19.470(5)	92.260(6)	1329.4(4)
Sm[a]	5.278(1)	12.751(1)	19.440(4)	92.408(5)	1307.2(4)
Eu	5.262(1)	12.712(1)	19.421(5)	92.471(6)	1297.9(4)
Gd	5.246(1)	12.667(1)	19.405(3)	92.53(1)	1288.1(3)
Tb	5.229(1)	12.626(1)	19.390(6)	92.540(6)	1278.9(5)
Dy	5.217(1)	12.572(1)	19.384(7)	92.665(6)	1270.0(5)
Y	5.202(1)	12.557(2)	19.384(3)	92.734(7)	1264.8(4)
Ho	5.200(1)	12.551(2)	19.387(3)	92.725(8)	1263.8(4)
Er	5.187(2)	12.522(6)	19.372(7)	92.79(2)	1256.8(9)
Tm	5.173(1)	12.485(1)	19.363(2)	92.841(7)	1249.0(3)
Yb	5.161(1)	12.463(2)	19.362(3)	92.93(2)	1243.8(4)
Lu	5.145(2)	12.437(4)	19.349(5)	92.98(3)	1236.4(7)

[a] ρ_x = 4.95 g/cm^3, ρ_{obs} = 4.92 g/cm^3.

dependence of decomposition temperatures of LiKLn_2 (MoO$_4$)$_4$ on the atomic number of a lanthanide has the maximum in the Gd–Tb–Dy region (Fig. 4c).

We failed to grow single crystals of LiMLn_2(MoO$_4$)$_4$ and refined the crystal structures of lanthanide-containing triple molybdates (as examples, neodymium containing phases were taken) with the Rietveld method using powder data [40]. We confirmed that LiMNd$_2$(MoO$_4$)$_4$ (M = K, Tl, Rb) were isostructural to LiRbBi$_2$(MoO$_4$)$_4$, whose structure has been determined from single crystal data [35]. Characteristic features of these structures (Fig. 5) are open layers formed by LnO$_8$ polyhedra and MoO$_4$ tetrahedra sharing common vertices. The adjacent layers are connected through MO$_{10}$ polyhedra and LiO$_6$ octahedra. Cations M^+ and Li$^+$ are in special positions at twofold axes. Cations R^{3+} occupy general positions [35,40].
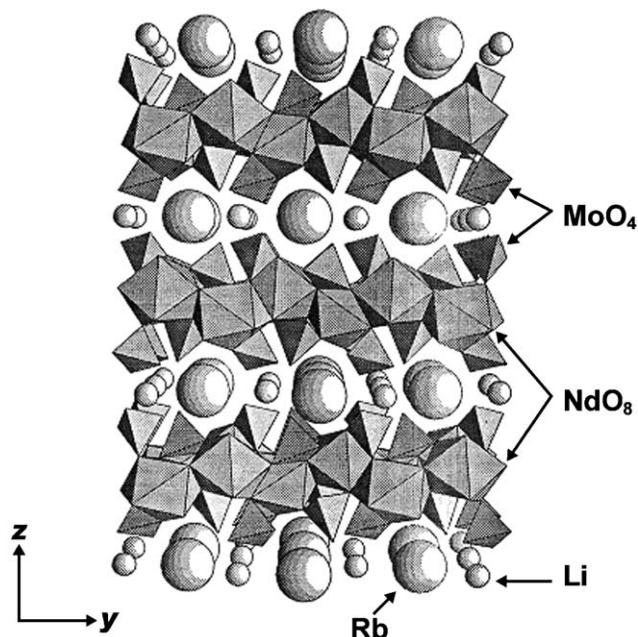
XRD powder patterns of LiKLn_2(MoO$_4$)$_4$ were indexed suggesting their structures being isotypical to LiKNd$_2$(MoO$_4$)$_4$ (monoclinic system, space group $C2/c$, Z = 4). The lattice parameters of these phases are given in Table 3.

We have given earlier the unit cell parameters of some triple molybdates LiKLn_2(MoO$_4$)$_4$ in a triclinic setting [2]. They may be reduced to the data presented in Table 3 with the transformation matrix (100)/(120)/(001).

It is known that CN = 8 is more characteristic for light rare-earths. Heavy lanthanides lean towards forming structures where their cations are 7 or 6-coordinated. Perhaps, it is just that explains troubles in
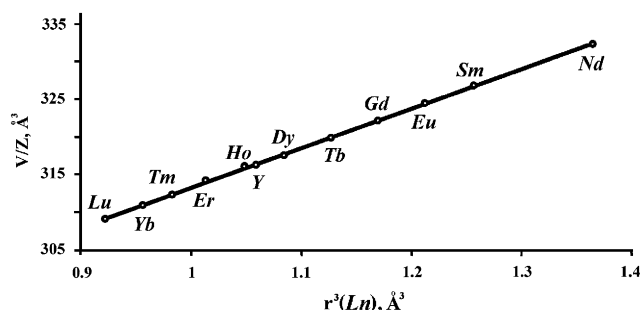
Fig. 6. V/Z dependence on $r^3(Ln)$ for a $LiKLn_2(MoO_4)_4$.

Table 4
Crystallographic characteristics of some triple molybdates $LiMLn_2$ $(MoO_4)_4$ (M = K, Tl, Rb)[a]

M	Unit cell parameters				
	a (Å)	b (Å)	c (Å)	β (deg)	V (Å)^3
Ln = Nd					
K	5.315(1)	12.857(1)	19.470(5)	92.260(6)	1329.4(4)
Tl	5.312(1)	12.936(1)	19.611(4)	92.659(5)	1346.3(4)
Rb	5.308(1)	12.970(1)	19.604(3)	92.467(4)	1348.4(3)
Ln = Sm					
K	5.278(1)	12.751(1)	19.440(4)	92.408(5)	1307.2(4)
Tl	5.277(1)	12.838(2)	19.595(5)	92.753(8)	1326.0(5)
Rb	5.276(1)	12.876(2)	19.579(7)	92.657(7)	1328.6(6)
Ln = Eu					
K	5.262(1)	12.712(1)	19.421(5)	92.471(6)	1297.9(4)
Tl	5.265(2)	12.799(2)	19.595(6)	92.906(6)	1318.7(7)
Rb	5.261(1)	12.839(1)	19.577(7)	92.716(6)	1320.8(5)

[a]Data for $LiMLn_2(MoO_4)_4$ (M = Tl, Rb) are taken from [3,5].

realization of the structure considered in the case of the heaviest Ln^{3+} (Yb, Lu).

As seen in Table 3, the lattice parameters a, b, c of $LiKLn_2(MoO_4)_4$ fall steadily throughout the rare-earth row while the monoclinic angle increases. The same tendencies in changing crystallographic characteristics are observed in the case of $LiMLn_2(MoO_4)_4$ (M = Tl, Rb) [3,5]. In all cases lanthanide contraction occurs as decrease of the unit cell volume along with fall of the lanthanide ion radius (Table 3, Fig. 6, [3,5]).

Substitution of potassium ion for a larger rubidium ion with the same rare-earth (Table 4) is accompanied by increases of b, c parameters and β angle; a parameter changes insignificantly but with a slight tendency toward decreasing. These tendencies break to some extent when non-alkaline metal M = Tl joins this series, but a steady increase of the unit cell volumes for $LiMLn_2(MoO_4)_4$ in the row K→Tl→Rb with M^+ radius growth keeps in all cases.

According to thermoanalytical data $LiKLn_2(MoO_4)_4$ (Ln = Sm–Tm, Y) possess no polymorphism. DTA curve of $LiKNd_2(MoO_4)_4$ shows a slight endothermic

effect at 510 °C which perhaps corresponds to a phase transition. Polymorphous transformations in a close temperature range (480–500 °C) were also found for $LiRbLn_2(MoO_4)_4$ (Ln = La, Ce) and $LiTlCe_2(MoO_4)_4$ [3,5].

4. Conclusions

By constructing the subsolidus phase diagrams of the systems Li_2MoO_4–K_2MoO_4–$Ln_2(MoO_4)_3$ (Ln = La, Nd, Dy, Er) existence of triple molybdates $LiKLn_2$ $(MoO_4)_4$ (Ln = Nd, Dy, Er) was confirmed. Compounds $LiKLn_2(MoO_4)_4$ was prepared for Ln = Nd–Lu, Y, their crystallographic and thermal characteristics were determined. A new low-temperature modification of $KDy(MoO_4)_2$ isotypical to triclinic α-$KEu(MoO_4)_2$ was revealed. It was shown that it being stabilized by Li^+ insertion in the structure.

References

[1] M.V. Mokhosoev, K.M. Khalbaeva, E.G. Khaikina, Z.I. Khazheeva, A.M. Frolov, Dokl. Phys. Chem. (Engl. Transl.) 312 (1990) 501.
[2] M.V. Mokhosoev, O.M. Basovich, E.G. Khaikina, Dokl. Chem. (Engl. Transl.) 316 (1991) 13.
[3] O.M. Basovich, E.G. Khaikina, Russ. J. Inorg. Chem. (Engl. Transl.) 39 (1994) 1353.
[4] K.M. Khalbaeva, E.G. Khaikina, Russ. J. Inorg. Chem. (Engl. Transl.) 45 (2000) 257.
[5] O.M. Basovich, E.G. Khaikina, E.V. Vasil'ev, A.M. Frolov, Russ. J. Inorg. Chem. (Engl. Transl.) 40 (1995) 1966.
[6] O.M. Basovich, E.G. Khaikina, Russ. J. Inorg. Chem. (Engl. Transl.) 45 (2000) 1409.
[7] F. Hoermann, Z. anorg. allg. Chem. 177 (1928) 145.
[8] I.N. Belyaev, Russ. J. Inorg. Chem. (Engl. Transl.) 6 (1961) 602.
[9] P.V. Klevtsov, S.V. Melnikova, R.F. Klevtsova, A.I. Kruglik, Sov. Phys. Crystallogr. (Engl. Transl.) 33 (1988) 692.
[10] V.K. Trunov, A.A. Evdokimov, T.P. Rybakova, T.A. Berezina, Russ. J. Inorg. Chem. (Engl. Transl.) 24 (1979) 93.
[11] P.V. Klevtsov, V.I. Protasova, L.Yu. Kharchenko, R.F. Klevtsova, Sov. Phys. Crystallogr. (Engl. Transl.) 18 (1973) 523.
[12] A.A. Evdokimov, V.V. Mishin, S.A. Smirnov, A.N. Pokrovsky, Zh. Neorg. Khim. 29 (1984) 2898 (in Russian).
[13] T.P. Rybakova, V.K. Trunov, Russ. J. Inorg. Chem. (Engl. Transl.) 18 (1973) 254.
[14] A.A. Evdokimov, A.A. Eliseev, V.A. Murashov, G.P. Khomchenko, Russ. J. Inorg. Chem. (Engl. Transl.) 26 (1981) 1659.
[15] T.P. Rybakova, V.K. Trunov, Zh. Neorg. Khim. 19 (1974) 1070 (in Russian).
[16] V.I. Protasova, L. Yu. Kharchenko, Zh. Neorg. Khim. 26 (1981) 2271 (in Russian).
[17] O.G. Potapova, V.I. Protasova, L.Yu. Kharchenko, Russ. J. Inorg. Chem. (Engl. Transl.) 32 (1987) 1703.

[18] W. Guertler, Z. anorg. und allg. Chem. 154 (1926) 439.
[19] A.M. Zakharov, "Fazovye diagrammy Dvoinykh i Troinykh Sistem". ["Phase Diagrams of Binary and Ternary Systems"], Metallurgiya, Moscow, 1978 (in Russian).
[20] V.K. Rybakov, V.K. Trunov, Russ. J. Inorg. Chem. (Engl. Transl.) 14 (1969) 1524.
[21] V.K. Trunov, T.P. Rybakova, Russ. J. Inorg. Chem. (Engl. Transl.) 15 (1970) 1577.
[22] B.M. Wanklyn, F.R. Wondre, J. Crystal Growth 43 (1978) 93.
[23] N.N. Bushuev, V.K. Trunov, A.B. Gizhinsky, Russ. J. Inorg. Chem. (Engl. Transl.) 18 (1973) 1523.
[24] P.V. Klevtsov, R.F. Klevtsova, J. Struct. Chem. (Engl. Transl.) 18 (1977) 339.
[25] B.M. Sokolovsky, A.A. Evdokimov, V.K. Trunov, Zh. Neorg. Khim. 22 (1977) 1499 (in Russian).
[26] P.V. Klevtsov, Bull. Soc. Fr. Mineral. Crystallogr. 92 (1969) 352.
[27] P.V. Klevtsov, L.P. Kozeeva, A.A. Pavlyuk, Kristallografiya 20 (1975) 1216 (in Russian).
[28] P.V. Klevtsov, L.P. Kozeeva, Kristallografiya 21 (1976) 316 (in Russian).
[29] V.K. Trunov, V.A. Efremov, Yu.A. Velikodny, Kristallokhimiya i Svoistva Dvoinykh Molibdatov i Volframatov. [Crystal Chemistry and Properties of Double Molybdates and Tungstates], Nauka, Leningrad, 1986 (in Russian).
[30] A.A. Evdokimov, V.A. Efremov, V.K. Trunov, I.A. Kleiman, B.F. Dzhurinsky, Soedineniya Redkozemelnykh Elementov. Molibdaty. Volframaty. [Rare-earth Compounds. Molybdates. Tungstates], Nauka, Moscow, 1991 (in Russian).
[31] JCPDS PDF-2 Data Base, Card # 52-1695.
[32] Y.-I. Kim, F. Izumi, J. Ceram. Soc. Jpn. 102 (1994) 401.
[33] R.F. Klevtsova, L.P. Kozeeva, P.V. Klevtsov, Sov. Phys. Crystallogr. (Engl. Transl.) 19 (1974) 89.
[34] D.Yu. Naumov, E.V. Boldyreva, J. Struct. Chem. (Engl. Transl.) 40 (1999) 86.
[35] R.F. Klevtsova, L.A. Glinskaya, V.I. Alekseev, K.M. Khalbaeva, E.G. Khaikina, J. Struct. Chem. (Engl. Transl.) 34 (1993) 789.
[36] R.F. Klevtsova, A.D. Vasil'ev, L.A. Glinskaya, A.I. Kruglik, N.M. Kozhevnikova, V.P. Korsun, J. Struct. Chem. (Engl. Transl.) 33 (1992) 443.
[37] I.I. Kiseleva, M.I. Sirota, R.I. Ozerov, T.P. Balakireva, A.A. Maier, Kristallografiya 24 (1979) 1277 (in Russian).
[38] Z.Ya. Pol'shchikova, V.K. Trunov, Russ. J. Inorg. Chem. (Engl. Transl.). 15 (1970) 587.
[39] R.D. Shannon, Acta Crystallogr. A 32 (1976) 751.
[40] V.A. Morozov, B.I. Lazoryak, V.A. Smirnov, V.V. Mikhailin, O.M. Basovich, E.G. Khaikina, Russ. J. Inorg. Chem. (Engl. Transl.) 46 (2001) 873.